

DEVELOPMENT OF A NEW FLEX-PLI LS-DYNA MODEL AND INVESTIGATIONS OF INJURY FROM VEHICLE IMPACT

Masahiro Awano

Isamu Nishimura

Mitsubishi Motors Corporation

Shinya Hayashi

JSOL Corporation

Japan

Paper Number 09-0088

ABSTRACT

A new flexible pedestrian legform impactor (Flex-PLI) has been developed by Japan Automobile Manufacturers Association, Inc. (JAMA) and Japan Automobile Research Institute (JARI).

The new Flex-PLI has good biofidelity as well as several knee ligament elongation measurement capabilities, three femur and four tibia bending moment measurement capabilities. For these reasons Flex-PLI is likely to be adopted for the future pedestrian Global Technical Regulation.

This presentation introduces a finite element model of the Flex-PLI for LS-DYNA and presents a CAE (Computer Aided Engineering) study that investigates Flex-PLI kinematic behaviour caused by impact with a vehicle. The new Flex-PLI LS-DYNA model was carefully created to ensure that every important detail was included. Geometries, masses and material properties of all parts were reproduced from drawings and inspection of the real components. Connectivity and component interaction within the model were determined by thorough experiments. Accurate prediction of injury indices and kinematic behaviour was achieved by correlation to JARI's static and dynamic calibration tests. A fine mesh was used while reasonable calculation cost assured by imposing an analysis time step of 0.9 micro seconds.

In this report, investigations by computer simulation of Flex-PLI deformation behaviour mechanisms during vehicle impact are presented.

INTRODUCTION

The increase of traffic accidents between pedestrians and vehicles is recognized as an ongoing serious problem. One approach to reduce pedestrian injuries is to improve the front structure of vehicles.

Pedestrian injury statistics from traffic accident databases accumulated in the USA, Germany, Japan and Australia show that pedestrian AIS 2-6 injuries occurred to the head in 31.4% of the cases and to the legs in 32.6% [1][2]. In the EU, protection of pedestrian lower legs has already been regulated in EEC2003/102 and assessed by EuroNCAP. These

use a rigid-bone type lower leg impactor produced by TRL.

JAMA and JARI have developed a new **Flexible Pedestrian Legform Impactor** (Flex-PLI) with improved biofidelity as well as more appropriate injury measurement capabilities. The 1st version of Flex-PLI was created in 2002 [3] and since then various technical evaluations have been carried out by the Flex-TEG (Flexible Pedestrian legform Impactor Technical Evaluation Group), conducted under GRSP/INF-PS-GR of the United Nations. JAMA and JARI have continued to improve and upgrade Flex-PLI, and in 2007 the 5th version, called Type GT (Flex-GT) was produced [4]. The Flex-GT has been verified worldwide to have excellent test repeatability and be sufficiently practical for use as a certification test tool [5][6].

From 2008 to 2009 the Flex-GT was upgraded to the 6th version, Type GTR (Flex-GTR) [7]. Flex-GTR is expected to have the same performance as Type GT and is planned to be the final design. It is likely to be used for the future pedestrian Global Technical Regulation.

In order to develop vehicles using Flex-PLI, the application of CAE is essential and must be very efficient. Therefore, in 2008, a Flex-GT LS-DYNA model development was started. In a second phase continuing to 2009, the Flex-GT model was further validated in real-vehicle impact scenarios and proven to be a highly accurate yet numerically stable model.

FLEX-GT LS-DYNA MODEL DEVELOPMENT

Model General Outline

Figure 1 shows the whole view of Flex-GT LS-DYNA model. The Flex-GT comprises an internal skeleton structure covered with a flesh material made up of layered neoprene and rubber sheets.

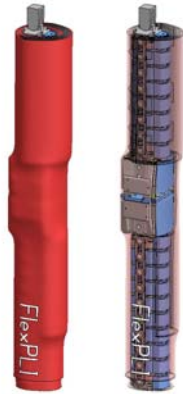


Figure 1. Flex-GT model whole view.

The mesh size and distribution in the Flex-GT model was developed over a series of concept phases in order to achieve sufficient accuracy at minimal calculation cost. The minimum mesh size of deformable parts was limited by imposing a 0.9micro second time step. Total elements amount to around 540,000 but deformable elements only to 220,000.

The geometry of the model was created not only from 2D drawings but also from long and detailed inspection of a physical impactor. The physical impactor was completely disassembled to measure accurately the size and weight of all components. The Flex-GT model is thus set up carefully to have the exact same mass distribution as the physical impactor.

Figure 2 shows the internal structure of Flex-GT. On the left is the LS-DYNA model, on the right is the physical impactor [8]. The internal structure is composed of three portions: femur, knee and tibia.

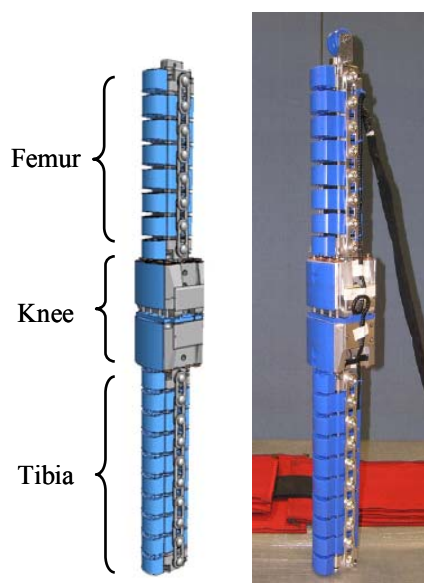


Figure 2. Flex-GT internal structure: LS-DYNA model and a physical impactor.

Bone cores form the fundamental structure inside the femur and tibia, and provide the flexibility and stiffness in those areas.

The knee joint is made up of two blocks connected by steel cables and springs which replicate ligaments in the real human knee. With this system, good biofidelic behaviour can be achieved without requiring replacement parts. The ligament layout is asymmetric because it represents a human right leg hit from the right side.

The Flex-GT model was developed using LS-DYNA Version 971 R3.2.1 [9].

Model Detailed Description

Bone Core Model - Figure 3 shows the femur and tibia bone cores. They were modelled using a purely elastic material because the real parts are made of strong glass fiber reinforced plastic (FRP) and assumed not to incur any permanent deformation (plastic strain) under normal loads. Young's Modulus was determined from 3-point bending static calibrations. Strain gauges, which in the real device are glued on the bone cores, were modelled by very weak spring elements attached using tied contacts. Three spring elements were attached to each side of the femur bone (at the same height on the tension and compression surfaces) and four to each side of the tibia, according to the specification of Flex-GT.

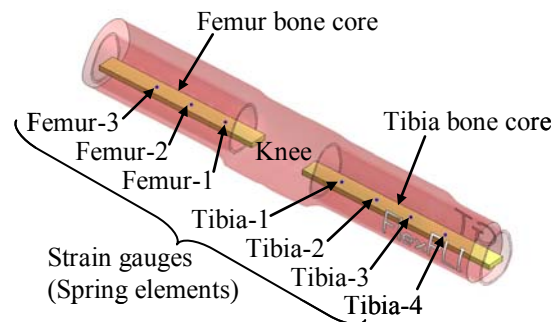


Figure 3. Bone cores and strain gauges.

Femur and Tibia Models - Figure 4 shows a section through the tibia model. The femur model has the same structure. The bone core lies down the middle of square section exterior housings which were are chained together by links down their flanks. The MC-nylon exterior housings were modelled using an elastic material and the aluminium core binders and connection bolts by a rigid material. Friction coefficients of the core binders and the connection bolts contacting on the bone cores were estimated from surface conditions of the real parts and then further tuned in the later calibration studies. Connection plates tie the exterior housing structures together and link together around connection bolts.

Accurate connectivity of the links was determined from detailed observation of the physical impactor.

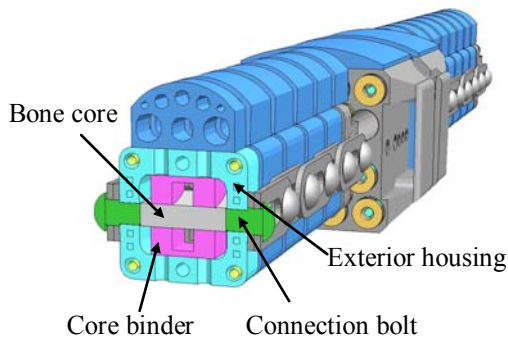


Figure 4. Exterior housing.

Figure 5 shows the connection between the femur and knee condyle model. The tibia is connected in a similar manner. The core binder at the end of the femur was attached to the knee condyle using a discrete beam element. The connection stiffness was set with reference to the physical components, and later revised in a correlation study during dynamic calibration.

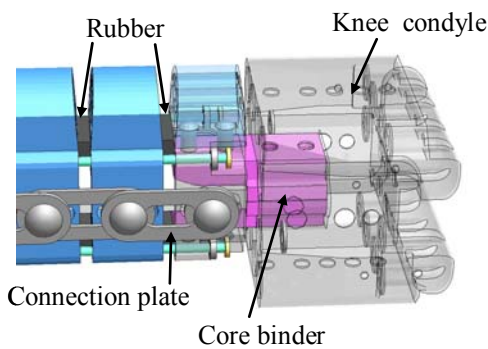


Figure 5. Connection of core binder and knee condyle.

Figure 6 shows the bending stopper cable model. This was modelled explicitly to behave in the same way as the physical impactor: the cable limits the total bend when the stopper contacts the exterior housings.

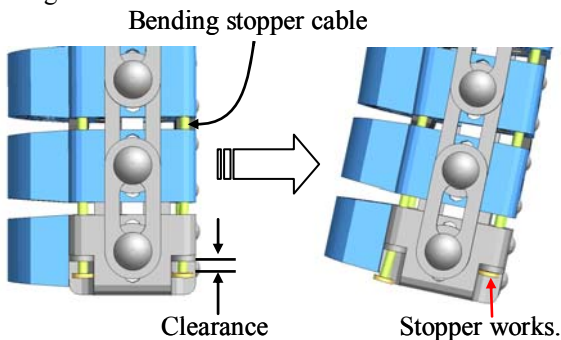


Figure 6. Bending stopper cable.

Knee Model - Figure 7 shows the model of the knee. The upper and lower knee condyles were modelled using a rigid material. The area contacting

the ligament cables was modelled with very fine mesh for accurate and stable interaction with the ligament cables. The MC-nylon contact face between upper and lower knee condyles was modelled using an elastic material. The convex impact faces were also modelled in a similar way.

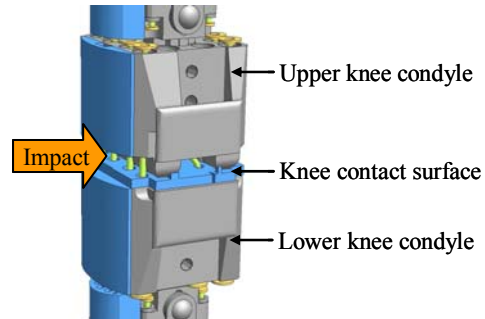


Figure 7. Knee whole view.

Figure 8 shows the knee ligament model. Four kinds of ligament cables: ACL (Anterior Cruciate Ligament), MCL (Medial Collateral Ligament), PCL (Posterior Cruciate Ligament) and LCL (Lateral Collateral Ligament), were created using very detailed and complicated modelling techniques. Ligament spring stiffness was determined from specifications and later calibrated during the correlation phase. The completed knee model was found to have good performance in predicting the varied kinematic behaviour of the real device.

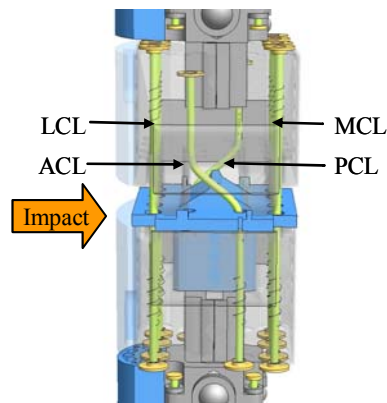


Figure 8. Knee ligament structure.

Figure 9 shows the model of the three knee potentiometers measuring extensions at ACL, MCL and PCL locations. These were modelled using weak spring elements: their deflections measure the same distance as the real wire potentiometers.

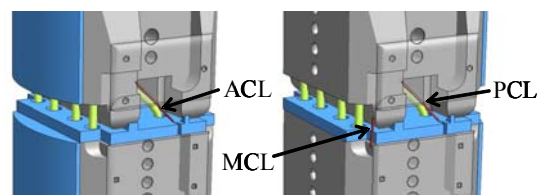


Figure 9. Knee potentiometers.

The knee joint system can flex in complicated kinematic modes: not only in bending but also in shear and torsion. It is designed to behave in the same way as a human knee. In particular, when it hits a curved area of the vehicle, a combined twist, shear and bend mode can often occur. Accurate realisation of all kinematic modes is vital for correct injury prediction and this has been achieved using detailed modelling techniques and thorough validation stages.

Flesh - Figure 10 shows the layered structure of neoprene and rubber sheets that form the flesh in the same way as the physical impactor (see also Figures 11, 12). Wide adhesive tape is used to hold the rubber sheets to the femur and this was modelled by membrane elements with realistic stiffness. Rate sensitive material properties of the neoprene and rubber were developed from accurate static and dynamic tests of production sheets.

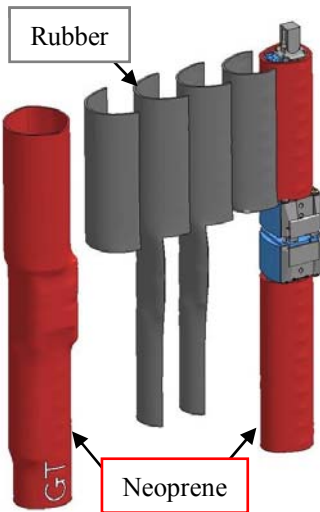


Figure 10. Layered sheets of flesh construction.



Figure 11. Flesh construction of Flex-GT model and physical impactor (Top).



Figure 12. Flesh construction of Flex-GT model and physical impactor (Bottom).

Model Calibrations

Bone Core Static Calibration - Simulations of 3-point bending static calibration tests for the femur and tibia bone cores [10] were performed and the Young's Modulus of the core adjusted to achieve the correct calibration stiffness (see Figures 13, 14).

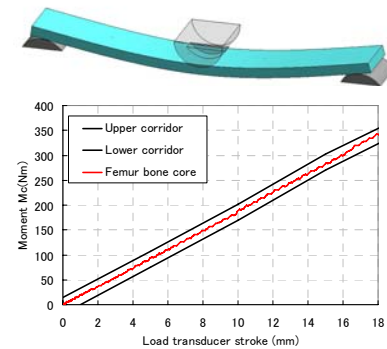


Figure 13. Femur bone core calibration result.

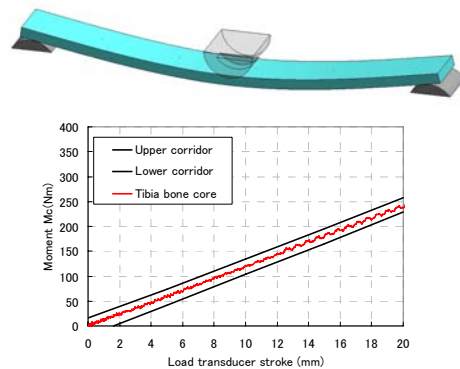


Figure 14. Tibia bone core calibration result.

The Flex-GT model is designed to be analyzed using explicit LS-DYNA, so these simulations were analyzed using the quasi-static method in explicit code. In this method the loading occurs over a very short period of time but care is taken to ensure that inertia effects are kept to a minimum and do not influence the result. It was found that correct geometries of the load transducer and support jigs were very important to get precise results. These methods were also used in the other quasi-static calibration studies.

During this stage, factors to convert strain gauge output (spring elements) into bending moments were calculated and set in the model.

Femur and Tibia Static Calibration – Figures 15 to 18 show the results of the 3-point bending static calibration analysis for the femur and tibia model assemblies [10]. The models were adjusted to satisfy calibration stiffness requirements, and the deflection modes compared to photos of the real tests (Figures 17, 18).

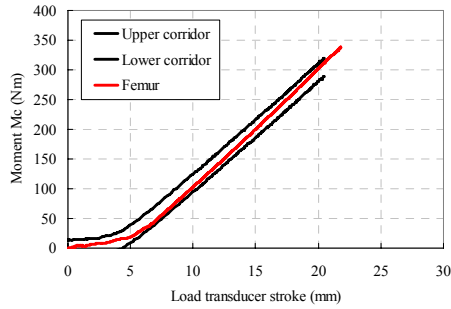


Figure 15. Femur static calibration result.

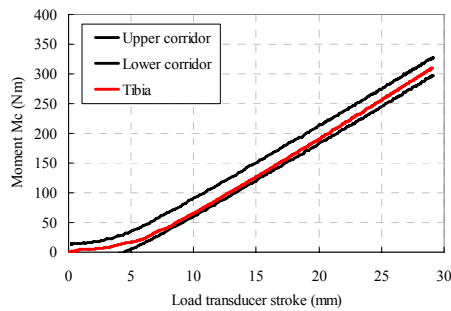


Figure 16. Tibia static calibration result.

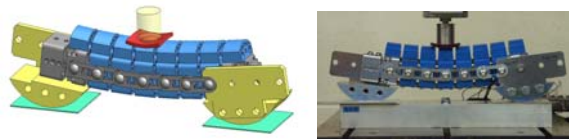


Figure 17. Femur deflection in static calibration

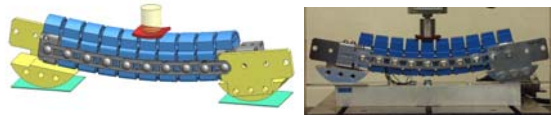


Figure 18. Tibia deflection in static calibration

Complicated support jigs attached to the both sides of the femur and tibia were modelled carefully since they influence the results.

According to the test specification, one sheet of neoprene is inserted between the load transducer and leg assembly. This deformed significantly because of its low stiffness and was often a cause of calculation instability. To avoid this problem, contact definitions and element size were modified many times. These stability modelling methods for the neoprene were also applied to the final flesh model.

Knee Static Calibration - Figures 19 and 20 show the results of the 3-point bending static calibration analysis for the knee model [10]. The model was adjusted to satisfy calibration stiffness

requirements, and the deflection mode compared to photos of the real test (Figure 20).

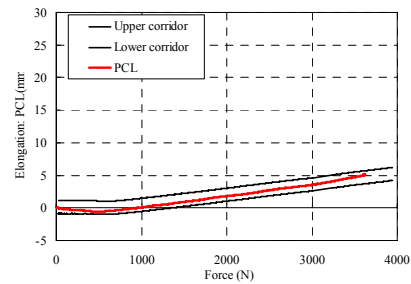
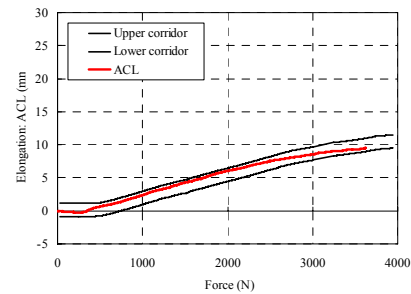
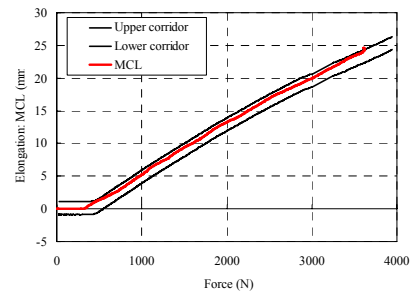
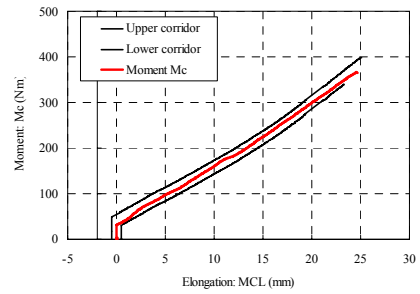


Figure 19. Knee static calibration result.

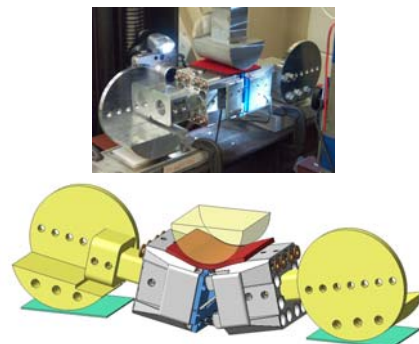


Figure 20. Knee deflection in static calibration

Assembly Dynamic Calibration – The whole internal structure of the Flex-GT was assembled from the calibrated femur, tibia and knee models and a model of the test jig created according to the dynamic calibration test specification. As shown in Figure 21, the top of the femur is connected to the jig via a pin joint and the leg is released to freely swing down from a position 15 degrees above horizontal.

Calibration requirements are defined by a corridor for peak injury of knee MCL, PCL and ACL elongations, three femur bending moments and four tibia bending moments [10]. The graphs in Figure 22 show that the Flex-GT model not only satisfies all calibration requirements but also predicts the rise and fall of injury over time with great accuracy. Figure 23 shows the model deformation at maximum MCL injury (maximum bend).

During this phase the femur, tibia and knee models were modified slightly so each static calibration test was reanalyzed and model recalibrated.

In the dynamic analysis set up, the Flex-GT leg initial position was set to be just impacting the jig and given an initial velocity. This method saves much calculation time by omitting the free drop phase. However the angular velocity at impact was not defined in the calibration specification. At first an attempt was made to calculate this theoretically but in the end a free drop simulation was performed to obtain the correct angular velocity.

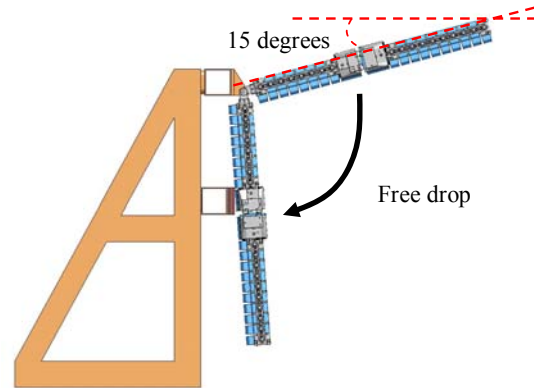


Figure 21. Dynamic calibration specification.

- Calibration corridor
- Test
- Simulation (LS-DYNA)

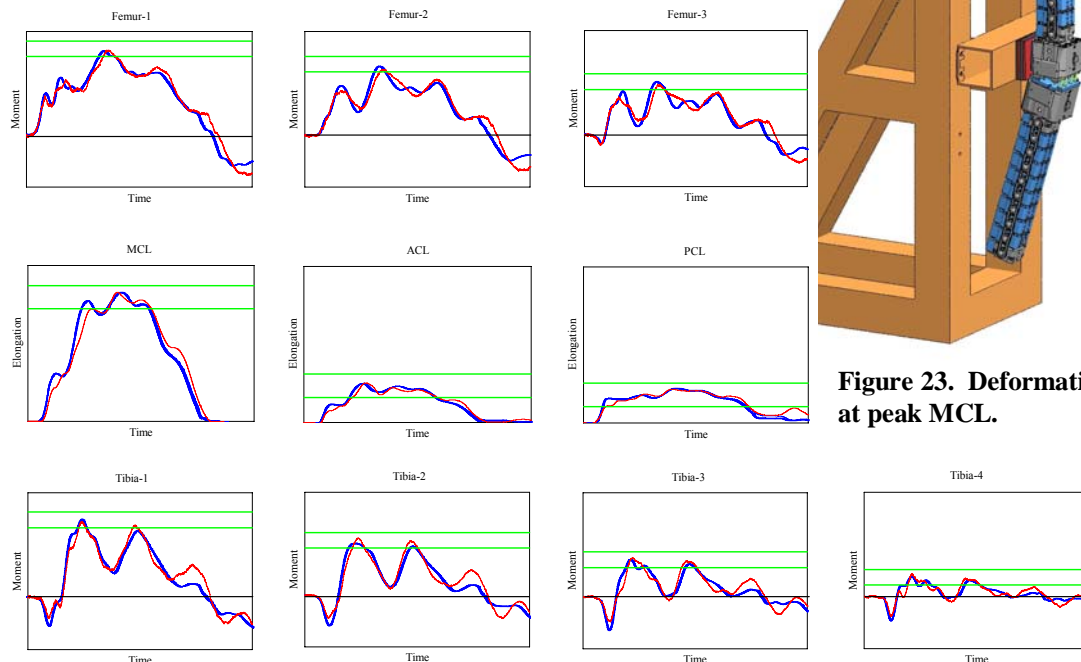


Figure 23. Deformation at peak MCL.

Figure 22. Dynamic calibration result: comparison of simulation and test.

FLEX-GT SIMPLIFIED CAR RIG IMPACT

In this study, a series of simplified car rig impacts were performed to validate the accuracy of the Flex-GT model. Figure 24 shows the simplified car rig test just before impact.



Figure 24. Simplified car rig test.

The simplified car rig was designed to represent the front structure of a vehicle. It comprises a BLE (Bonnet Leading Edge) plate, bumper and spoiler. The BLE is bent steel plate; the bumper and spoiler are PP(polypropylene) expanded foam blocks (see Figure 25).

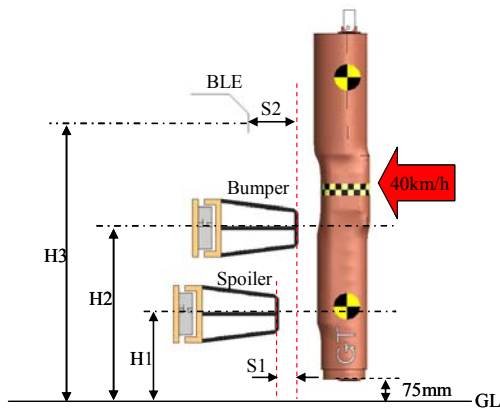


Figure 25. Simplified car rig setback and height.

The BLE, bumper and spoiler were positioned with setback and height as shown in Table.1. This represents a Type A sedan vehicle. The test was performed at an impact velocity of 40km/h and ground clearance of 75mm.

Table 1.
Setback and height conditions (mm)

TEST ID	S1	S2	H1	H2	H3
B02	50	130	Sedan type A		

A high accuracy simplified car rig model was created. A detailed mesh model of the BLE plate and PP foam blocks was made and their structural response correlated to dynamic impact tests. The model was set up as shown in Figure 26 so that the impact velocity, ground clearance and impactor position

were exactly like test conditions. In this test, four accelerometers (femur upper, knee upper, knee lower and tibia lower) were specially added on the internal structure of the Flex-GT (see Figure 27).

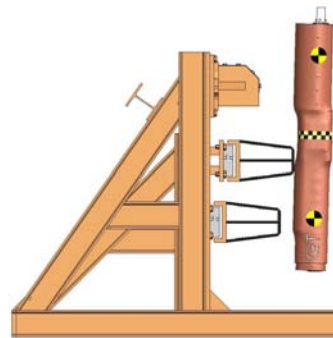


Figure 26. Simplified car rig LS-DYNA model.

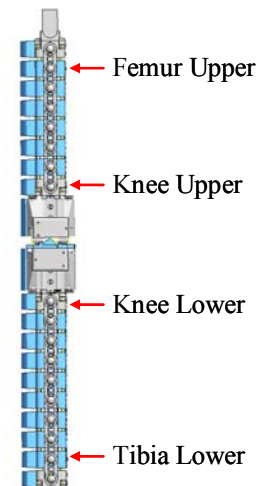


Figure 27. Accelerometers added on Flex-GT.

Figure 28 shows injury graphs of test and the simulation results. The peak values and graphical trends are well correlated. However, the simulation predicted peak femur moments 5-10msec earlier than the test. This is thought to be caused by a small difference in BLE mounting stiffness or deformation mode.

Figure 29 shows a comparison of Flex-GT kinematics. The test result was taken from high-speed film.

Figure 30 shows the acceleration pulses and graphs of acceleration vs. stroke. The kinematics of the model is nearly identical to test. The femur upper acceleration predicted from 25-32msec was a little higher than test. As described above, this is thought to be related to the accuracy of the BLE fitting model.

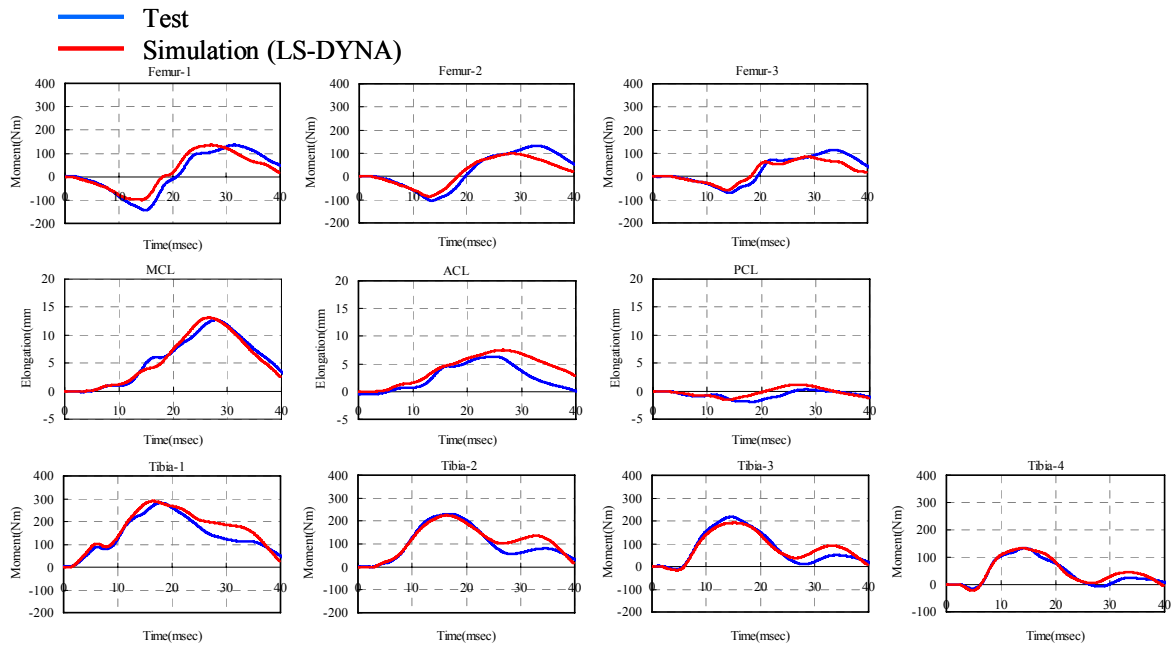


Figure 28. Flex-GT injury time history curves.

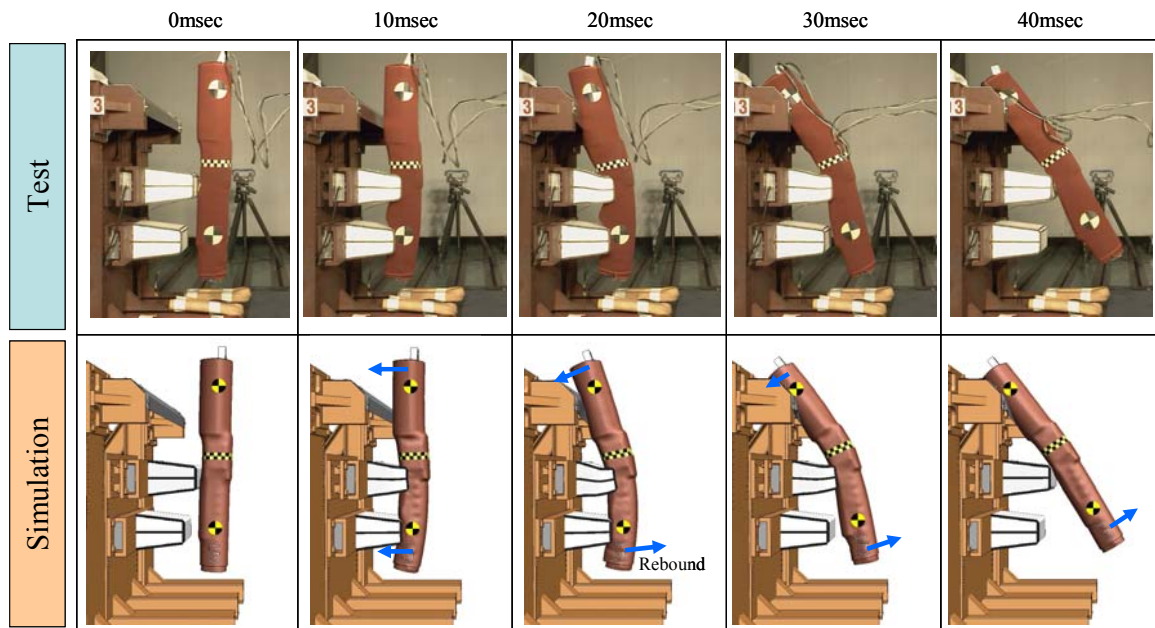


Figure 29. Flex-GT deformation mode.

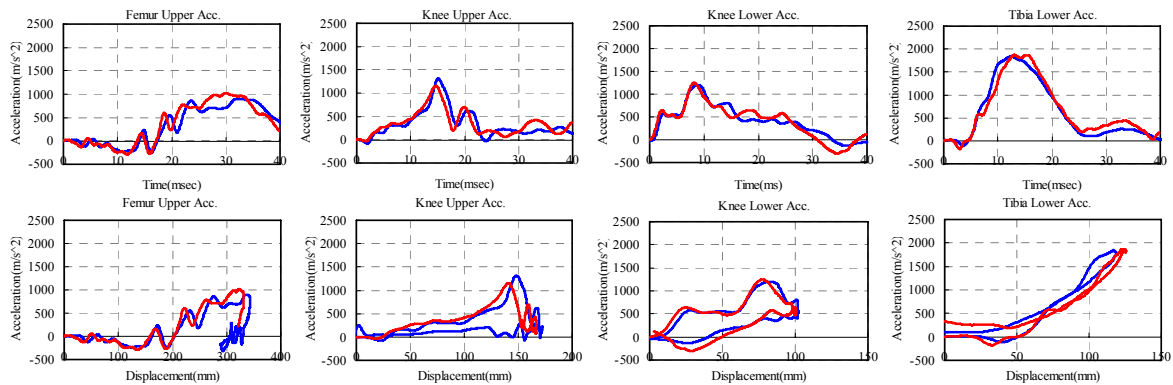


Figure 30. Flex-GT acceleration and displacement curves.

Flex-GT Injury Investigation

In this study, the Flex-GT injury mechanisms which occur in the simplified car rig test (see Figures 28 to 30) are investigated and some ideas for reducing these injuries are studied.

First, the lower knee contacts the bumper and the knee lower acceleration rises sharply. Soon after, the tibia contacts the spoiler which is located 50mm back from the bumper. At just 15msec the tibia starts to rebound by unloading forces from the bumper and the spoiler. At this time the lower tibia is moving like the curl of a whip and the tibia lower acceleration reaches a maximum.

The femur starts to contact the BLE at around 15msec, and the peak knee upper acceleration happens at that time. The BLE is positioned 150mm backward from the bumper. At 30msec the femur starts to rebound from the BLE and the femur upper acceleration reaches a maximum. Overall, the Flex-GT rotates forward and finally leans on the BLE. This is mainly caused by the setback differences of the BLE and the spoiler.

The peak MCL occurs at approximately 27msec while Flex-GT is still rotating forward. The maximum tibia moment, 289Nm, occurs at Tibia-1 near the bumper, at 15msec when the bumper reaction force becomes greatest. The maximum femur moment, 136Nm, occurs at Femur-1 at 30msec, when the BLE reaction force reaches its peak.

Ways to reduce Flex-GT injuries are discussed in the following section. As described above, the peak MCL occurs during the overall rotation of Flex-GT. It is considered likely that MCL is related to the rebounding properties of the bumper and spoiler and the stiffness of BLE.

There are two simple ideas to reduce the MCL.

- Control the kinematic behaviour of Flex-GT.
- Absorb more energy within the vehicle front structure (without adversely affecting performance in other crashes).

Better kinematic behaviour means less femur forward displacement, achieved using a stiff BLE, and/or greater tibia rearward motion by a larger rebound off the spoiler. Also, the rebounding stiffness of the bumper should be less than the spoiler because reaction forces from the bumper contribute more to knee bending.

However, these countermeasures require raising forces on the femur and tibia and might lead to increase in bending moments. The bending moments are measured all along the femur and tibia (see Figure 3), so any countermeasure loads must be distributed

carefully.

This problem suggests that it is necessary to carefully control load balance and timing on the femur and tibia as well as the distribution of energy absorption within the vehicle structure and Flex-GT.

In order to solve such a complicated problem with so many input parameters, an optimization method is recommended. CAE is a very efficient way to obtain an optimized solution in a short period of time and at reasonable cost. Also, CAE is able to provide a lot of detailed data: reaction force time histories, visualisation of load paths through the vehicle structure, insight into the Flex-GT kinematic modes and detailed knee bending behaviour (See Figure 31). This data is needed to clearly understand the mechanisms that cause leg injury. It is impossible to get such data relying only on real experiments. Furthermore, this method can be used on vehicles in the early design stages, before any real prototypes exist.

The Flex-GT model is considered an essential tool in the development of effective pedestrian protection technologies.

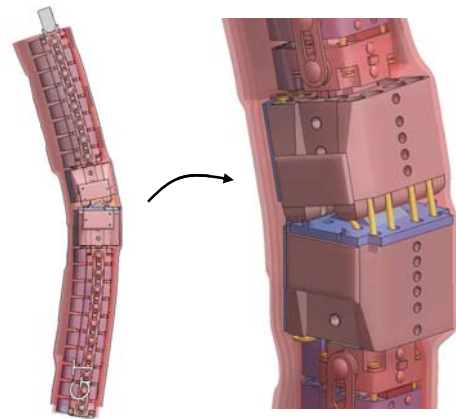


Figure 31. Flex-GT deformation mode.

Further Simplified Car Rig Tests

As shown in Table 2, a total of 6 impact cases were performed using the simplified car rig in various setback and height configurations. In all cases, the model showed excellent agreement with tests. The Flex-GT model was thus validated to a high accuracy level under similar impact conditions with real vehicles. Also, these results themselves were very useful to investigate the influence of vehicle front structure layout upon the Flex-GT kinematic behaviour.

Table 2.
All test case conditions (mm)

CASE ID	S1	S2	H1	H2	H3
B01	0	130	Sedan type A		
B02	50	130			
B03	100	130			
B04	0	130	SUV type A		
B05	50	130			
B07	50	130	SUV type B		

FULL VEHICLE MODEL FLEX-GT IMPACT

Figures 32 and 33 show two impact simulations with a full vehicle and the resulting stress distribution.

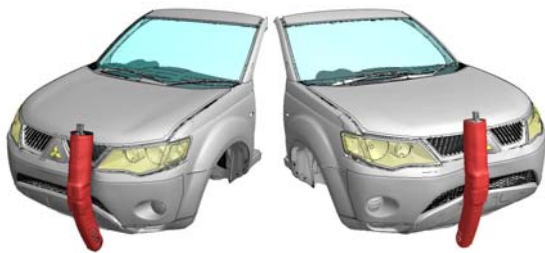


Figure 32. Full vehicle model results.

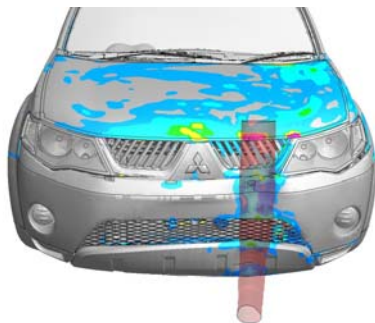


Figure 33. Stress distribution in vehicle.

The Flex-GT LS-DYNA model was confirmed to be highly robust under several full vehicle impact conditions and the calculation cost deemed very reasonable at current computing standards. Overall, the Flex-GT model is considered highly suited to CAE vehicle development.

FLEX-GTR MODEL DEVELOPMENT PLAN

An effort to upgrade Flex-GT LS-DYNA model into Flex-GTR is currently underway. Part of the upgrade includes changes to the knee ligament system [11], but most of structure and performance of Flex-GTR is reported to be similar to the Flex-GT. Therefore the modelling techniques and methods employed in developing Flex-GT model can be directly applied to Flex-GTR, ensuring the same high level of accuracy and realism.

CONCLUSION

A Flex-GT LS-DYNA model has been successfully developed and the following results were obtained:

- 1) A high accuracy Flex-GT LS-DYNA model was developed that satisfies all calibration requirements. In particular, excellent correlation of injury graphs was achieved in the dynamic calibration test.
- 2) Thorough validation was achieved using a series of simplified car rig impacts at 40km/h. By accurately predicting the same trends as test, the Flex-GT model is confirmed to have sufficient accuracy and high performance for use in vehicle development analysis.

ACKNOWLEDGEMENT

The authors would like to show grateful appreciation to the engineers at JARI for their cooperation and help in understanding the physical Flex-GT impactor, and also for executing the precise calibration and simplified car rig tests used in this study. They would also like to thank Richard Taylor of Arup for advice and support.

REFERENCES

- [1] Mizuno Y.: "Summary of IHRA Pedestrian Safety WG Activities (2005) – Proposed Test Methods to Evaluate Pedestrian Protection Afforded by Passenger Cars", Paper Number 05-0138 ESV (2005)
- [2] Konosu A.: "Development of Flexible Pedestrian Legform Impactor (Flex-PLI) and Introduction of Flex-PLI Technical Evaluation Group (Flex-TEG) Activities", <http://www.sae.org/events/gim/presentations/2008konosu1.pdf>, SAE Government/Industry Meeting (2008)
- [3] Konosu A. and Tanahashi M.: "Development of a biofidelic pedestrian legform impactor: Introduction of JAMA-JARI legform impactor ver. 2002. Proc", 18th International Technical Conference on the Enhanced Safety of Vehicle, Paper No. 378 (2003)
- [4] UN/ECE/WP29/GRSP/INF-GR-PS/Flex-TEG: "Information on Flexible Pedestrian Legform Impactor Type GT (Flex-GT)", TEG-033 (2007)
- [5] UN/ECE/WP29/GRSP/INF-GR-PS/Flex-TEG: "Flex GT Testing of US Vehicles", TEG-063 (2008)
- [6] UN/ECE/WP29/GRSP/INF-GR-PS/Flex-TEG: "Flex-GT: Repeatability and reproducibility of assembly certification and inverse test results",

TEG-051 (2007)

[7] UN/ECE/WP29/GRSP/INF-DOC: “Status Report on Flexible Pedestrian Legform Impactor Technical Evaluation Group (Flex-TEG) Activities”, GRSP-44-28 (2008)

[8] UN/ECE/WP29/GRSP/INF-GR-PS/Flex-TEG: “Report on Tests with the Flexible Pedestrian Legform Impactor Flex GT α and Flex GT”, TEG-043 (2007)

[9] Hallquist J. O.: “LS-DYNA Keyword User’s Manual Version 971” (2007)

[10] UN/ECE/WP29/GRSP/INF-GR-PS/Flex-TEG: “Flex-GT Full Calibration Test Procedures”, TEG-047 (2007)

[11] UN/ECE/WP29/GRSP/INF-GR-PS/Flex-TEG: “FLEX-PLI-GTR Development Mechanical Design”, TEG-054 (2008)